

Preparation and properties of ZrB₂-YAG-Al₂O₃ ceramics

Jie-Guang Song^{a,*}, Gang-Chang Ji^a, Shi-Bin Li^a, Yang-Liang Li^a, Da-Ming Du^a, Yin-Yan Ju^a and Lian-Meng Zhang^b

^aSchool of Mechanical and Materials Engineering, Jiujiang University, Jiujiang 332005, China

^bState Key Laboratory of Advanced Technology for Materials Synthesis and Processing, Wuhan University of Technology, Wuhan 430070, China

ZrB₂, YAG and Al₂O₃ are widely applied because of some excellent properties, but ZrB₂ is easily oxidized in high-temperature air. To achieve better properties in ZrB₂ ceramics, high-density ZrB₂-YAG-Al₂O₃ ceramics were prepared. Below 1000 °C, the shrinkage of ZrB₂-YAG-Al₂O₃ ceramics is less than that of ZrB₂-YAG ceramics. From 1000 °C to 1600 °C, the second largest shrinkage occurs. Above 1600 °C, the shrinkage of ZrB₂-YAG-Al₂O₃ ceramics is more than that of ZrB₂-YAG ceramics. The fracture toughness of sintered ceramics from coated raw materials is higher than that of sintered ceramics with mixed raw materials with the same phases and phase content, the fracture toughness of ZrB₂-YAG-Al₂O₃ ceramics is higher than that of ZrB₂-YAG ceramics with the same raw materials. The weight gain of all types of ceramics is increased with all increase in the oxidation temperature, the weight gain of ceramics is reduced with all increase in the YAG-Al₂O₃ content and Al₂O₃ proportion, especially above 1500 °C.

Key words: ZrB₂ ceramics, Sintering shrinkage, Fracture toughness, Oxidation.

Introduction

Zirconium diboride (ZrB₂) has attracted substantial interest because of its extreme chemical and physical properties, such as, high melting point, superior hardness and low electrical resistance. ZrB₂ has several applications such as in Hall-Heroult cell cathodes for electrochemical processing of aluminium, evaporation boats, crucibles for handling molten metals, thermowell tubes for steel refining, thermocouple sleeves for high-temperature use, nozzles, plasma electrodes, or as adispersoid in metal and ceramic-matrix composites for heaters and igniters [1-4]. However, ZrB₂ is easily oxidized in high-temperature air which impacts its high-temperature strength, restricts its applied range [5, 6]. Some excellent oxidation-resistance materials are considered as assistant phases for ZrB₂ materials to prepare ZrB₂ composite materials to improve the high-temperature performance of ZrB₂ materials, such as Al₂O₃-ZrB₂, SiC-ZrB₂, LaB₂-ZrB₂, and ZrO₂-ZrB₂ [7-9].

Yttrium aluminium garnet (YAG or Y₃Al₅O₁₂) has a cubic garnet structure and is of great interest as a high-temperature engineering material, due to its high-temperature strength coupled with low creep rate [10-14], which indicates that YAG ought to be a suitable matrix or reinforcing phase [15, 16].

To give ZrB₂ ceramics better oxidation resistance, in this paper, high-density ZrB₂-YAG-Al₂O₃ ceramics were prepared and the properties of these ceramics were investigated.

*Corresponding author:
Tel :+86 792 8313990
Fax:+86 792 8311239
E-mail: songjieguang@yahoo.com.cn

Materials and Experiment

Analytical grade aluminum nitrate, yttrium nitrate, ammonia and commercially available ZrB₂ powder (99.5% in purity) were used. ZrB₂ coated with Al₂O₃-Y₂O₃ composite powder was synthesized by a co-precipitation method [17]. Superfine Al₂O₃-Y₂O₃ composite powder was synthesized with aluminum nitrate, yttrium nitrate and ammonia via a co-precipitation method. Superfine Al₂O₃-Y₂O₃ composite powder was calcined at 1000 to obtain superfine YAG powder. YAG was mixed into ZrB₂ powder to form a mixed raw material. Then the composite raw materials were encased in a graphite mould, sintered, demoulded and tested. Different ceramics were prepared with spark plasma sintering (SPS) (Table 1). A process flow diagram is shown in Fig. 1.

ZrB₂-YAG-Al₂O₃ ceramics were prepared by SPS (Mode: SPS-1050, Japan) and oxidation treated in a furnace (Mode: Nabertherm LHT04, Germany). Phase analysis was performed by X-ray powder diffraction (XRD) (Model: D/Max-RB, Japan). Microstructure analysis was performed by scanning electron microscopy (SEM) (Model: JSM-5610LV, Japan). Element analysis was performed

Table 1. Types of ceramics

Ceramics	YAG : Al ₂ O ₃ (mol)	Phase
Z		ZrB ₂
Z-Y		ZrB ₂ + YAG
Z-YA	1 : 1	ZrB ₂ + YAG + Al ₂ O ₃
Z-Y3A	1 : 3	ZrB ₂ + YAG + Al ₂ O ₃
Z-Y6A	1 : 6	ZrB ₂ + YAG + Al ₂ O ₃

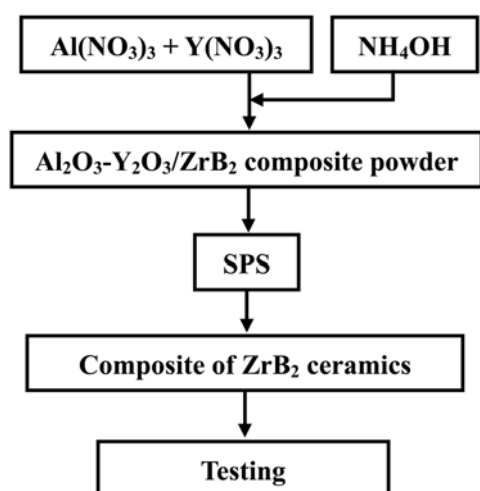


Fig. 1. The process flow diagram of preparing YAG- ZrB_2 multi-phase ceramics.

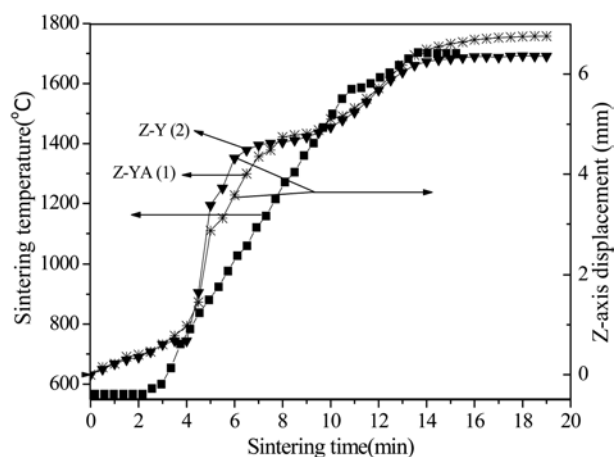


Fig. 2. Sintering shrinkage curves of Z-20wt%YA and Z-20wt%Y ceramics.

with an electron probe microanalysis system (EPMA) (Model: JXA-880R, Japan).

Results and Discussion

Sintering behavior of ZrB_2 -YAG- Al_2O_3 ceramics

The sintering curve of the ceramics prepared by SPS is shown in Fig. 2. The Z-axis displacement shows the shrinkage state of the ceramic body during the sintering process, the value of the Z-axis displacement increases, which indicates the ceramic body is shrinking, on the contrary, the ceramic body is expanding. The Z-axis displacement (1) and Z-axis displacement (2) show the shrinkage state of sintered Z-YA ceramics and Z-Y ceramics, respectively. The shrinkage curves (1) and (2) are similar, however, there are differences. Below 1000 °C, the shrinkage of Z-YA ceramics is less than that of Z-Y ceramics, because the shrinkage is caused by forming YAG from Al_2O_3 and Y_2O_3 from 700 °C to 950 °C [18]. From 1000 °C to 1600 °C, YAG melts and fills the space between ZrB_2

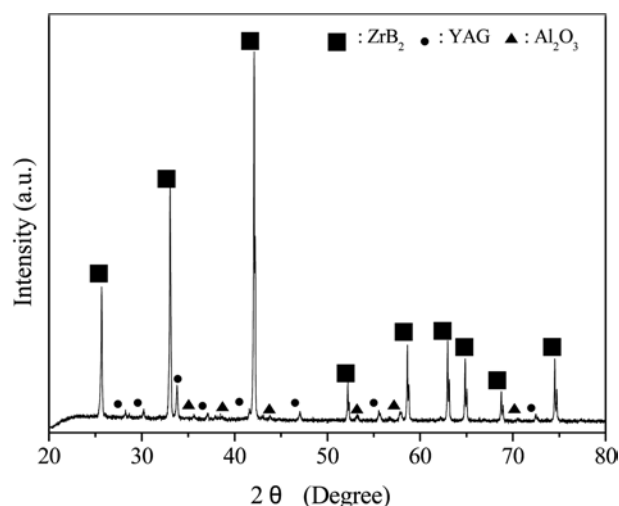


Fig. 3. XRD of ZrB_2 -YAG- Al_2O_3 ceramics.

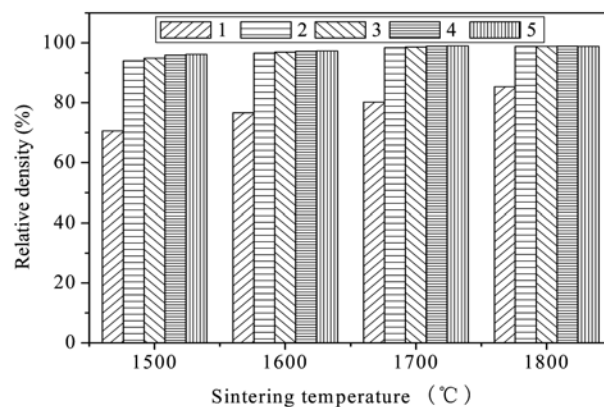


Fig. 4. Effect of sintering temperature on the relative density of ceramics (1-Z ceramics, 2-Z-30 wt%Y ceramics, 3-Z-30 wt%YA ceramics, 4-Z-30 wt%Y3A ceramics and 5-Z-30 wt%Y6A ceramics).

particles in the SPS system [19, 20], which brings about the second largish shrinkage. Above 1600 °C, the shrinkage of Z-YA ceramics is more than that of Z-Y ceramics, because the shrinkage is caused by Al_2O_3 diffusion [21]. The XRD of ZrB_2 -YAG- Al_2O_3 ceramics prepared with the SPS process at 1700 °C is shown in Fig. 3. The relative densities of ceramics are shown in Fig. 4, which indicate that the relative density is increased with an increase in the sintering temperature, the phase type and the proportion of Al_2O_3 . The effect of the YA content on the microstructure of Z-YA ceramics is shown in Fig. 5.

Mechanical property of ZrB_2 -YAG- Al_2O_3 ceramics

The fracture toughness of sintered ceramics from coated ZrB_2 powder and mixed ZrB_2 powder at a sintering temperature of 1700 °C, a sintering pressure for 20 MPa and a holding time for 4 minutes is shown in Fig. 6, which indicates that the fracture toughness of sintered ceramics with coated raw materials is higher than that of sintered ceramics with mixed raw materials with the

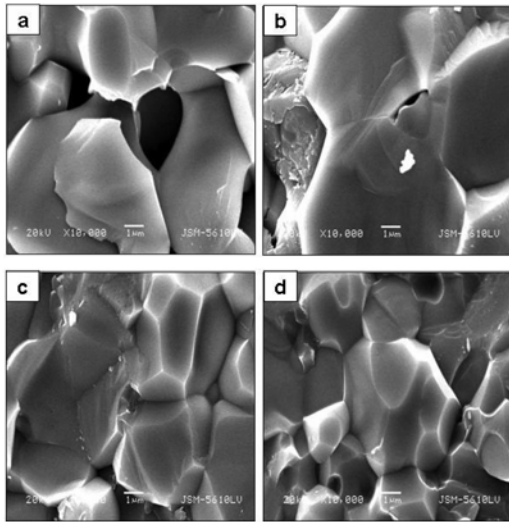


Fig. 5. Effect of YA content on microstructure of Z-YA ceramics (a-10 wt%, b-20 wt%, c-30 wt% and d-40 wt%).

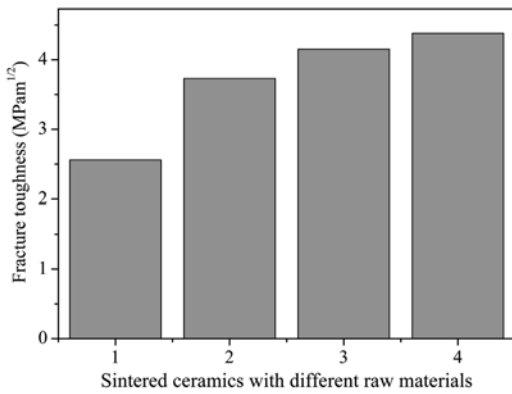


Fig. 6. Effect of raw materials on fracture toughness of ceramics (1-Mixing 30 wt%Y, 2-Mixing 30 wt%Y6A, 3-Coating 30 wt%Y and 4-Coating 30 wt%Y6A).

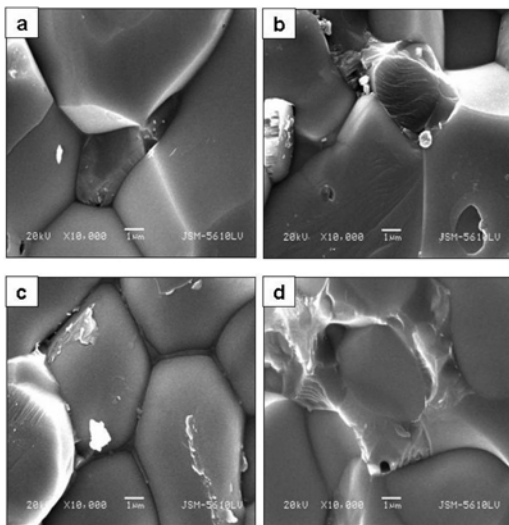


Fig. 7. Effect of raw materials on the microstructure of ceramics (a-Mixing 30 wt%Y, b-Mixing 30 wt%Y6A, c-Coating 30 wt%Y and d-Coating 30 wt%Y6A).

same phases and phase contents, the fracture toughness of Z-YA ceramics is higher than that of Z-Y ceramics. Because the YAG phase is situated in the space between the ZrB₂ particles after sintering with mixed raw materials by SPS (Fig. 7(a) and (b)), however, the YAG phase is situated on the crystal boundaries among the ZrB₂ particles after sintering the coated raw materials (Fig.7 (c) and (d)). In the later case YAG as the reinforce phase is homogeneously dispersed, which makes the reinforce effect with coated raw materials better than that with mixed raw materials. From Fig. 7, the ZrB₂ grain size is apparent, the ZrB₂ grain size is more homogeneous and finer with coated raw materials than that with mixed raw materials, because the reinforced phase may arrest the growth of

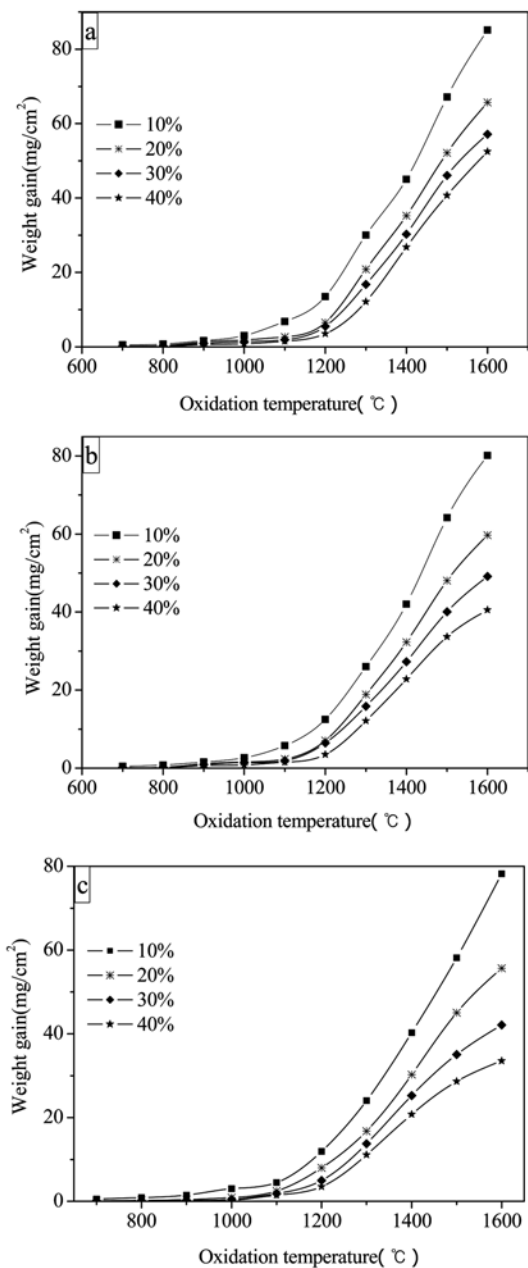


Fig. 8. Effect of oxidation temperature on weight gain of ceramics (a-Z-YA, b-Z-Y3A and c-Z-Y6A).

the ZrB_2 grains during the sintering process [22]. The fine grain size helps to increase the mechanical properties of YAG- ZrB_2 multi-phase ceramics. The mechanical properties of YAG- Al_2O_3 composite materials are higher than that of single phase YAG and Al_2O_3 materials. [23]

Oxidation resistance of ZrB_2 -YAG- Al_2O_3 ceramics

The weight gain of different ceramics after being oxidized at different oxidation temperatures for 1 hour is shown in Fig. 8, which indicates the weight gain of all types of ceramics is increased with an increase in the oxidation temperature. Also the weight gain of ceramics is reduced with an increase in the YAG- Al_2O_3 content and Al_2O_3 proportion, especially above 1500 °C. The effect of the oxidation temperature on the weight gain of ceramics is decided by the relative density of ceramics. However, factors such as the effect of YAG- Al_2O_3 content and YAG: Al_2O_3 ratio on the weight gain of ceramics are not just on the

relative density of ceramics, but also on the chemical reaction of ZrB_2 reactions with O_2 to form B_2O_3 [24], B_2O_3 reacts with Al_2O_3 to form $Al_{18}B_4O_{33}$ (Fig. 9). $Al_{18}B_4O_{33}$ melts and coats the surfaces of the ceramics to form a protection layer giving oxidation resistance of the ceramics at high temperatures [25] (Fig. 10). XRD patterns of ceramics with different Al_2O_3 contents after being oxidized at 1600 °C for 1 hour are shown in Fig. 11, which indicates the $Al_{18}B_4O_{33}$ content of the oxidized surfaces of ceramics are increased with an increase in the proportion of Al_2O_3 , which means the thickness of oxidation resistance layer is increased. SEM of an oxidized Z-40 wt%Y6A ceramic sample is shown in Fig. 12.

Conclusion

(a) The shrinkage of ZrB_2 -YAG- Al_2O_3 ceramics and ZrB_2 -YAG ceramics is similar, however, there are differences.

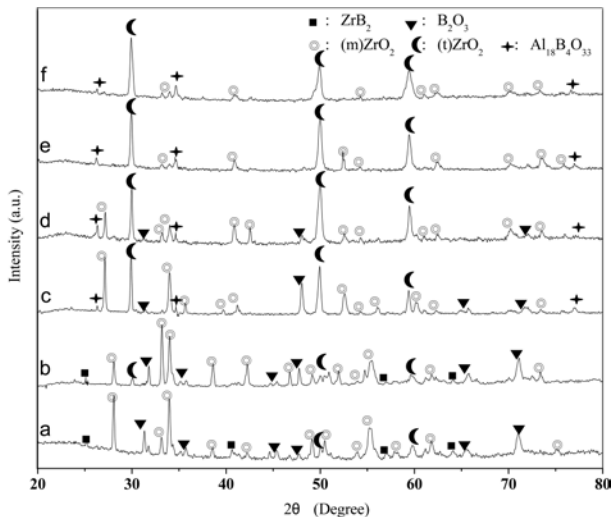


Fig. 9. Effect of oxidation temperature on the phase production in of Z-40 wt%YA ceramics (a-1100 °C, b-1200 °C, c-1300 °C, d-1400 °C, e-1500 °C and f-1600 °C).

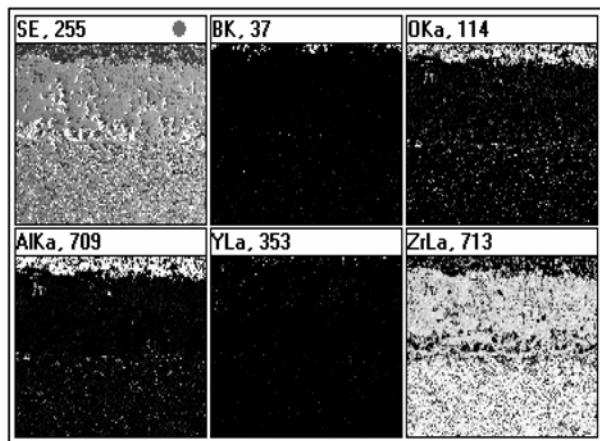


Fig. 10. Element distribution of ZrB_2 -40 wt%Y6A ceramics after being oxidized at 1600 °C for 1 hour.

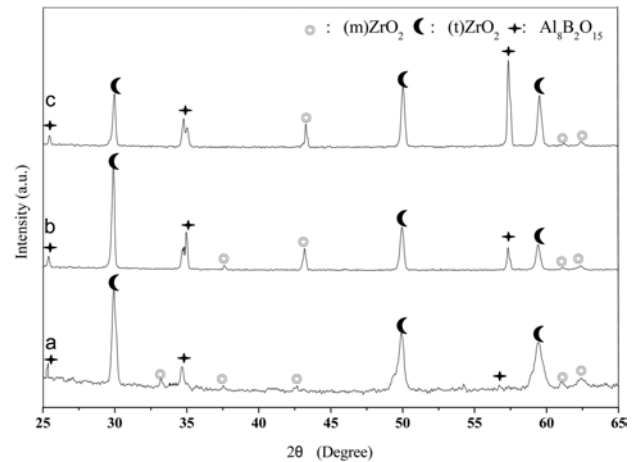


Fig. 11. XRD of surfaces of different ceramics after being oxidized at 1600 °C for 1 h (a-Z-40 wt%YA, b-Z-40 wt%Y3A and c-Z-40 wt%Y6A).

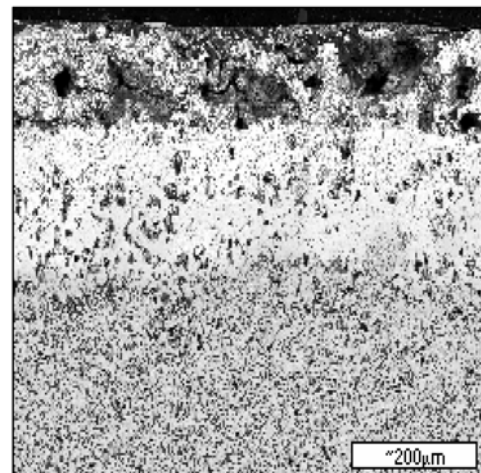


Fig. 12. Effect of oxidation temperature on the oxidation layer of ZrB_2 -40 wt%Y6A ceramic sample after being oxidized at 1600 °C for 1 hour.

Below 1000 °C, the shrinkage of ZrB₂-YAG-Al₂O₃ ceramics is less than that of ZrB₂-YAG ceramics. From 1000 °C to 1600 °C, a second large shrinkage occurs is caused. Above 1600 °C, the shrinkage of ZrB₂-YAG-Al₂O₃ ceramics is more than that of ZrB₂-YAG ceramics.

(b) The fracture toughness of sintered ceramics from coated raw materials is higher than that of sintered ceramics with mixed raw materials with the same phases and phase content, and the fracture toughness of ZrB₂-YAG-Al₂O₃ ceramics is higher than that of ZrB₂-YAG ceramics with the same raw materials.

(c) The weight gain of all type of ceramics is increased with an increase of the oxidation temperature, the weight gain of ceramics is reduced with an increase of the YAG-Al₂O₃ content and Al₂O₃ proportion, especially above 1500 °C.

Acknowledgments

The authors are thankful for the financial support provide by the Science Found for Young Scholars of the Educational Department of Jiangxi Province, China (No.GJJ09595), and for the apparatus provide by The Center for Materials Testing and The Functionally Gradient Material (FGM) Research Laboratory of Wuhan University of Technology, China.

References

1. S.C. Zhang, G.E. Hilmas, and W.G. Fahrenholtz, *J. Am. Ceram. Soc.* 89 (2006) 1544-1550.
2. S.M. Zhu, W.G. Fahrenholtz, G.E. Hilmas, and S.C. Zhang, *Mater. Sci. Eng. A* 459 (2007) 167-171.
3. F. Monteverde, A. Bellosi, and S. Guicciardi, *J. Eur. Ceram. Soc.* 22 (2002) 279-288.
4. D. Sciti, S. Guicciardi, and A. Bellosi, *J. Am. Ceram. Soc.* 89 (2006) 2320-2322.
5. I.B. Bankovskaya, M.P. Semov, and A.E. Lapshin, *Glass Phys. Chem.* 31 (2005) 433-438.
6. A.L. Chamberlain, W.G. Fahrenholtz, and G.E. Hilmas, *J. Am. Ceram. Soc.* 89 (2006) 450-456.
7. G.J. Zhang, Z.Y. Deng, N. Kondo, J. F. Yang, and T. Ohji, *J. Am. Ceram. Soc.* 83 (2000) 2330-2332.
8. A. Bellosi, F. Monteverde, and D. Sciti, *Int. J. Appl. Ceram. Tech.* 3 (2006) 32-40.
9. F. Monteverde and A. Bellosi, *Solid State Sci.* 7 (2005) 622-630.
10. A. Fernandez and J. Somers, *J. Mater. Sci.* 38 (2003) 2331-2335.
11. M.B. Kakade, S. Ramanathan, and S.K. Roy, *J. Mater. Sci. Lett.* 21 (2002) 927-929.
12. F. Ivanuskas, A. Kareiva, and B. Lapcun, *J. Math. Chem.* 37 (2005) 365-372.
13. X. Li, Q. Li, J.Y. Wang, and S.L. Yang, *J. Alloy. Comp.* 421 (2006) 298-302.
14. M. Ono, Y. Waku, and K. Habicht, *Appl. Phys. A* 74 (2002) 73-75.
15. R.M. Laine, J. Marchal, H.P. Sun, and X.Q. Pan, *Adv. Mater.* 17 (2005) 830-833.
16. S.J. Wang, Y.B. Xua, P.X. Lua, C.F. Xu, and W. Cao, *Mater. Sci. Eng. B* 127 (2006) 203-206.
17. J.G. Song, L.M. Zhang, J.G. Li, and J.R. Song, *J. Reinf. Plast. Comp.* 26 (2007) 139-145.
18. N. Zhang, Q.K. Cai, and H.Q. Ru, *J. Rare Earth.* 23 (2005) 299-303.
19. M. Omori, *Mater. Sci. Eng. A* 287 (2000) 183-188.
20. Y. Xiong, Z.Y. Fu, Y.C. Wang, and F. Quan, *J. Mater. Sci.* 41 (2006) 2537-2539.
21. Y.M. Kong, S. Kim, and H.E. Kim, *J. Am. Ceram. Soc.* 82 (1999) 2963-3031.
22. H.Z. Wang, L. Gao, W.Q. Li, and H. Kawaoka, *J. Inorg. Mater.* 16 (2001) 169-172.
23. L. Gao, W.Q. Li, and H.Z. Wang, *J. Inorg. Mater.* 15 (2000) 1107-1110.
24. A. Rezaie, W.G. Fahrenholtz, and G.E. Hilmas, *J. Am. Ceram. Soc.* 89 (2006) 3240-3245.
25. M. Brach, D. Sciti, and A. Balbo, *J. Eur. Ceram. Soc.* 25 (2005) 1771-1780.